RNA (1995), *1*:584–597. Cambridge University Press. Printed in the USA.

Prp16p, Slu7p, and Prp8p interact with the 3′ splice site in two distinct stages during the second catalytic step of pre-mRNA splicing

JAMES G. UMEN and CHRISTINE GUTHRIE

Department of Biochemistry and Biophysics, University of California—San Francisco, San Francisco, California 94143, USA

ABSTRACT

For the second catalytic step of pre-mRNA splicing to occur, a 3′ splice site must be selected and juxtaposed with the 5′ exon. Four proteins, Prp16p, Slu7p, Prp17p, Prp18p, and an integral spliceosomal protein, Prp8p, are known to be required for the second catalytic step. *prp8-101*, an allele of *PRP8* defective in 3′ splice site recognition, exhibits specific genetic interactions with mutant alleles of the other second step splicing factors. The *prp8-101* mutation also results in decreased crosslinking of Prp8p to the 3′ splice site. To determine the role of the step-two-specific proteins in 3′ splice site recognition and in binding of Prp8p to the 3′ splice site, we performed crosslinking studies in mutant and immunodepleted extracts. Our results suggest an ordered pathway in which, after the first catalytic step, Prp16p crosslinks strongly to the 3′ splice site and Prp8p and Slu7p crosslink weakly. ATP hydrolysis by Prp16p affects a conformational change that reduces the crosslinking of Prp16p with the 3′ splice site and allows stronger crosslinking of Prp8p and Slu7p. Thus, the 3′ splice site appears to be recognized in two stages during the second step of splicing. Strong 3′ splice site crosslinking of Prp8p and Slu7p also requires the functions of Prp17p and Prp18p. Therefore, Prp8p and Slu7p interact with the 3′ splice site at the latest stage of splicing prior to the second catalytic step that can currently be defined, and may be at the active site.

Keywords: UV crosslinking; U5 snRNP; yeast

INTRODUCTION

Nuclear pre-mRNA splicing involves the recognition and removal of introns from messenger RNA precursors. Five small ribonucleoproteins (U1, U2, U4, U5, and U6 snRNPs), together with multiple accessory proteins, recognize and assemble onto intron-containing RNAs in an ordered fashion to form the spliceosome and carry out the two transesterification reactions that characterize pre-mRNA splicing (see below for reviews). In the first chemical step, the 2′ hydroxyl of an internal (branch site) adenosine attacks the 5′ splice site phosphodiester bond to generate the lariat intermediate and free 5′ exon; in the second chemical step, the 3′ hydroxyl of the free 5′ exon attacks the 3′ splice site phosphodiester bond, forming ligated exons and an excised lariat intron.

These reactions require accurate identification and juxtaposition of splice sites. Although a great deal has been learned about this process for the first catalytic step of splicing, much less is known about 3′ splice site selection and the second catalytic step (Green, 1991; Guthrie, 1991; Rymond & Rosbash, 1992; Moore et al., 1993; Madhani & Guthrie, 1994a). 3′ Splice sites in most organisms contain a pyrimidine-rich tract upstream of an invariant AG dinucleotide at the 3′ splice junction. Moreover, a specific interaction between the first and last guanosine residues in introns plays an important functional role in 3′ splice site utilization (Parker & Siliciano, 1993). In mammals, the pyrimidine tract is recognized by a factor, U2AF, that is required at an early stage in spliceosome assembly (Zamore & Green, 1991). Later, the pyrimidine tract is bound by PSF (*P*TB associated splicing *f*actor), which is required for the second catalytic step (Gozani et al., 1994). In both *Saccharomyces cerevisiae* and mammals, U5 snRNA has been shown to base pair with exon sequences adjacent to the 3′ splice site; however, the lack of sequence conservation in these sequences suggests that this interaction does not normally play a major determinative role in 3′ splice site selection (Newman &

Reprint requests to: Christine Guthrie, Department of Biochemistry and Biophysics, University of California—San Francisco, San Francisco, California 94143, USA; e-mail: guthrie@socrates.ucsf.edu.

Norman, 1991, 1992; Wyatt et al., 1992; Cortes et al., 1993; Sontheimer & Steitz, 1993; Madhani & Guthrie, 1994a).

The U5 snRNP-associated protein Prp8p was originally identified from a temperature-sensitive mutant allele, *prp8-1*, that blocks splicing prior to the first catalytic step in vitro and in vivo (Lossky et al., 1987; Jackson et al., 1988; Brown & Beggs, 1992). Recently, however, we identified a novel allele, *prp8-101*, that is specifically defective for 3′ splice site selection. This allele impairs recognition of the uridine tract preceding the 3′ splice site and defines a function for Prp8p at the second catalytic step of splicing in vivo (Umen & Guthrie, 1995). Site-specific UV crosslinking suggests that Prp8p mediates 3′ splice site selection through direct binding to the 3′ splice site (Teigelkamp et al., 1995a; Umen & Guthrie, 1995).

In addition to the factors mentioned above, genetic screens in *S. cerevisiae* have identified four proteins that are required specifically for the second catalytic step: Prp16p, Slu7p, Prp17p, and Prp18p. These proteins are "exchangeable" because they can be removed from in vitro splicing reactions and then added back to complement pre-assembled spliceosomes (Vijayraghavan & Abelson, 1990; Schwer & Guthrie, 1991; Horowitz & Abelson, 1993a; Athar & Schwer, 1995; Jones et al., 1995). Additionally, *PRP16*, *PRP17*, *PRP18*, and *SLU7* share a unique set of genetic interactions with each other but not with other splicing factors, suggesting a physical or functional association of the encoded proteins (Frank et al., 1992; Jones et al., 1995). Originally identified as a suppressor of a branch site mutation, *PRP16* belongs to a family of RNA-dependent ATPases, the so called DExH box proteins (Couto et al., 1987; Burgess et al., 1990; Schmid & Linder, 1992). Prp16p binds to the spliceosome after the first catalytic step of splicing; it then promotes an ATP-dependent conformational change that leads to protection of the 3′ splice site from oligonucleotide-directed RNase H cleavage (Schwer & Guthrie, 1991, 1992a). Whether this protection is due to Prp16p or other splicing factors is not known.

SLU7 was identified in a screen for mutants that are *s*ynthetically *l*ethal with *U5* snRNA (Frank et al., 1992). Although Slu7p does not appear to be stably associated with U5 or other snRNPs (D.N. Frank, unpubl. obs.), the protein contains a sequence motif ($CX_2CX_4HX_4C$), termed a "zinc knuckle," that is implicated in retroviral RNA binding (Frank & Guthrie, 1992 and references therein). Interestingly, an allele of *SLU7*, *slu7-1*, affects 3′ splice site selection, suggesting a possible RNA binding site for the protein (Frank & Guthrie, 1992).

Prp17p and Prp18p are encoded by nonessential genes and absence of either causes a partial block to the second step of splicing in vitro (Vijayraghavan & Abelson, 1990; Frank et al., 1992; Horowitz & Abelson, 1993b; Jones et al., 1995). Whereas Prp16p and Prp17p act at, or prior to, an ATP-requiring stage of splicing (Schwer & Guthrie, 1991; Jones et al., 1995), Prp18p and Slu7p do not require ATP to promote the second catalytic step (Horowitz & Abelson, 1993a; Athar & Schwer, 1995; Jones et al., 1995). Thus, Prp16p/Prp17p and Prp18p/Slu7p define at least two stages in the second step of splicing, one ATP-dependent and one ATP-independent.

Here we investigate the in vitro phenotype of *prp8-101*. We find that the mutant protein causes a block to the second catalytic step of splicing and is impaired in 3′ splice site crosslinking. The *prp8-101* mutant also displays specific genetic interactions with alleles of *PRP16*, *SLU7*, *PRP17*, and *PRP18*, establishing a functional relationship between Prp8p and these second step splicing factors. We utilize site-specific UV crosslinking to test whether the exchangeable second step splicing factors interact with the 3′ splice site, and to determine the timing of these interactions relative to that of Prp8p. We find that the 3′ splice site is recognized in at least two distinct stages. The first is characterized by strong 3′ splice site crosslinking of Prp16p and weaker crosslinking of Slu7p and Prp8p. After hydrolysis of ATP by Prp16p, Prp8p and Slu7p crosslinking to the 3′ splice site increases, whereas Prp16p crosslinking is diminished. Strong 3′ splice site crosslinking of Prp8p and Slu7p also requires the functions of Prp17p and Prp18p. Thus, Prp8p and Slu7p interact with the 3′ splice site at the closest stage of splicing prior to catalysis that can currently be defined.

RESULTS

In vitro analysis of the *prp8-101* mutant

Previously, we demonstrated that the *prp8-101* allele of *PRP8* causes a specific defect in 3′ splice site uridine tract recognition (Umen & Guthrie, 1995). Furthermore, we utilized a site-specifically labeled in vitro splicing substrate (XL7) and UV crosslinking to show that wild-type Prp8p crosslinks to the 3′ splice site in active spliceosomes (Fig. 1) (Umen & Guthrie, 1995). XL7 contains a point mutation (AG to GG) at the 3′ splice site that slows the kinetics of the second step and enhances crosslinking of Prp8p. We wished to determine whether the *prp8-101* allele causes a block to the second step of splicing in vitro and how the Prp8p–3′ splice site interaction is affected in the mutant strain. To test this, we prepared splicing extract from an epitope-tagged *prp8-101* strain (see the Materials and methods) and examined splicing and 3′ splice site crosslinking. In the *prp8-101* mutant extract, XL7 undergoes the first step of splicing at a similar efficiency compared with the wild-type extract. However, there is a block to the second catalytic step (Fig. 2A). This block is partial when the 3′ splice site dinucleotide is wild type (AG) (data not shown). We consistently ob-

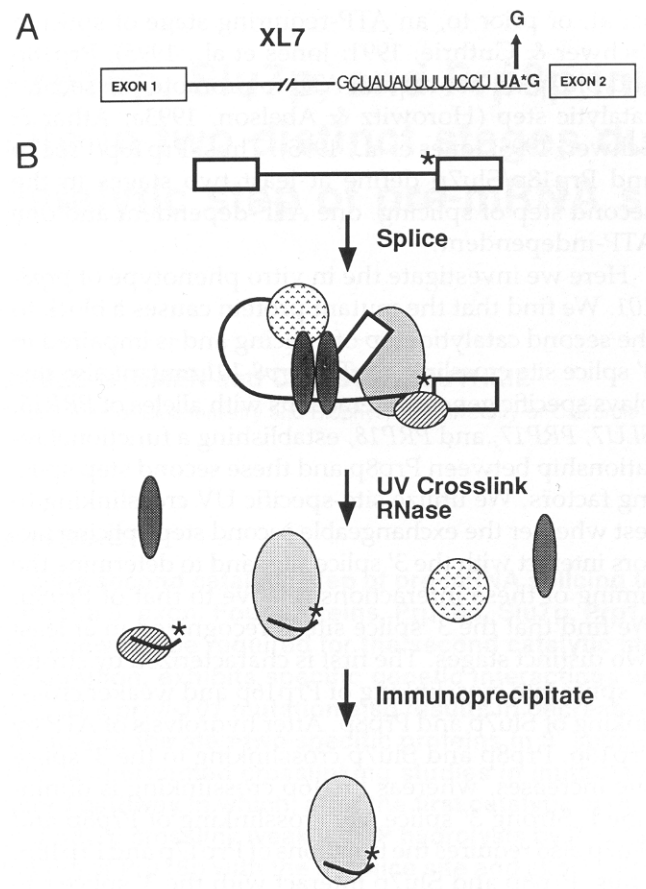

FIGURE 1. Strategy for analyzing 3′ splice site binding proteins. **A:** Schematic of XL7 in vitro splicing substrate. The 3′ splice site nucleotides are shown with the A to G point mutation and a single-labeled phosphate depicted by a * symbol. The 15-nt RNase T1 digestion product is underlined. **B:** XL7 is incubated in splicing extract and bound proteins are UV crosslinked. After digestion with RNase T1, only 3′ splice site bound proteins will be labeled and specific proteins can be isolated by immunoprecipitation.

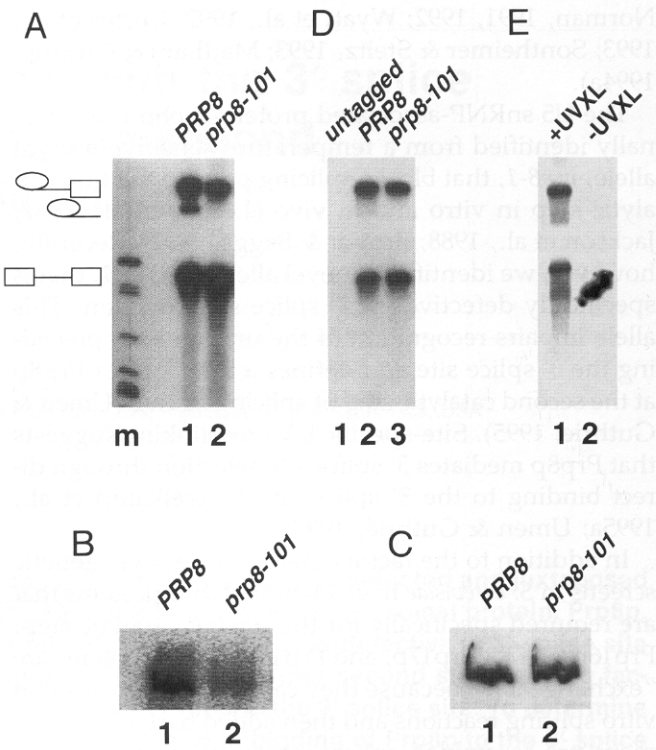

FIGURE 2. Analysis of 3′ splice site crosslinking in *prp8-101* strains. **A:** Splicing of XL7 in epitope-tagged *PRP8* (lane 1) and epitope-tagged *prp8-101* (lane 2) extracts. *Hpa* II-digested pBR322 markers are in lane m. Products of splicing are presented as line drawings to the left. **B:** Phosphorimage analysis of the crosslinked and immunoprecipitated Prp8p from A. **C:** Immunoblot analysis of the epitope-tagged Prp8p from B. **D:** Native immunoprecipitation of spliceosomes from A with anti-HA antibodies (lanes 2 and 3) and a wild-type, non-epitope-tagged extract in lane 1. **E:** Denaturing immunoprecipitation of wild-type, epitope-tagged Prp8p from reaction in A with (lane 1) and without (lane 2) UV crosslinking.

served a 2–4-fold reduction in Prp8p–3′ splice site crosslinking with the mutant *prp8-101* extract (Fig. 2B). Immunoblot analysis of the crosslinked samples indicated that similar quantities of protein were immunoprecipitated in each reaction (Fig. 2C). Furthermore, native immunoprecipitation of spliceosomes from wild-type and mutant extracts revealed that similar amounts of Prp8p are associated with precursor and lariat intermediate (Fig. 2D, lanes 2 and 3).

Interestingly, in contrast to previously reported results (Whittaker et al., 1990; Teigelkamp et al., 1995b), we detect very little association of Prp8p with excised lariat in this experiment. Even upon long exposure of the autoradiograph in Figure 2D, the proportion of excised lariat to lariat intermediate is greatly reduced in the immunoprecipitate versus the total splicing reaction (Fig. 2A, lane 1 versus Fig. 2D, lane 2). This may be due to differences between the two splicing substrates utilized, a difference in epitope accessibility in complexes containing excised lariat versus lariat intermediate and precursor, or differences in spliceosome disassembly rates in the respective splicing extracts. To test the second possibility, we crosslinked Prp8p to XL7 in a splicing reaction and analyzed Prp8p–XL7 crosslinking by denaturing immunoprecipitation (see the Materials and methods) (Fig. 2E). This experiment yields a similar profile of precipitated RNA species as the native immunoprecipitation. We conclude that in our extracts, Prp8p is primarily associated with precursor and lariat intermediate and only a small fraction could be associated with excised lariat. The discrepancy with previous results is either due to differences in the two substrates that were utilized or to differences in spliceosome disassembly rates. Our result further suggests that the Prp8p–3′ splice site interaction is altered or destabilized after the second catalytic step.

Genetic interactions between *PRP8* and other second step splicing factors

Synthetic lethal analysis has proven useful in de novo identification of interacting splicing factors and in func-

tionally grouping known splicing factors (Frank et al., 1992; Liao et al., 1993; Ruby et al., 1993; Wells & Ares, 1994). Mutant alleles of the second step splicing proteins encoded by *PRP16*, *SLU7*, *PRP17*, and *PRP18* exhibit synthetic lethality with each other but not with mutant alleles of proteins required for the first step of splicing (Frank et al., 1992). Because the *prp8-101* allele behaves specifically as a second step mutant both in vivo and in vitro, we tested whether it interacts genetically with mutant alleles of second step splicing genes. In principle, just as first step splicing factors fall into different genetic subgroups based on common biochemical functions, the same could be true of second step splicing factors; that is, *prp8-101* might define its own subgroup, or might be related in function to the other second step factors.

We employed a novel method for constructing and analyzing double mutants of *prp8-101* or *prp8-1* and alleles of both first and second step splicing mutants (Fig. 3A,B). This method involves the direct construction and analysis of double mutant strains via integrative transformation rather than the more laborious indirect analysis of meiotic progeny. It is particularly useful for rapidly screening one or two mutants against a large set of test strains. Either *prp8-101* or *prp8-1* were introduced into test strains carrying a chromosomal or plasmid-borne *prpx* mutation and a *URA3*-marked plasmid bearing a wild-type copy of the same *PRPX* gene. Selection against the *URA3-PRPX* plasmid with the drug 5-fluoro-orotic acid (5FOA) yields a double mutant *prp8 prpx* strain (Fig. 3B). Failure to grow on 5FOA indicates that the double mutant strain is inviable and that the mutations are synthetically lethal. Compared with *prp8-101* strains, which grow at near wild-type rates and are mildly temperature sensitive, *prp8-1* strains grow slowly and are highly temperature sensitive. Therefore, *prp8-1* served as a good control for specificity in these experiments.

We analyzed three first step splicing mutants (*prp2-1*, *prp3-1*, and *prp24-6*) and at least one allele of all the second step splicing factors (*prp16-101*, *prp16-2*, *prp16-301*, *prp17-1*, *prp17-2*, *prp18-1*, *slu7-1*, and *slu7-ccss* [double mutation in the "zinc knuckle" (Frank & Guthrie, 1992)]). Strikingly, we found that *prp8-101* is synthetically lethal with at least one allele of all the second step splicing factors, but displays no genetic interactions with the first step mutants (Fig. 3C). For *PRP16*, we only observed synthetic lethality with a cold-sensitive

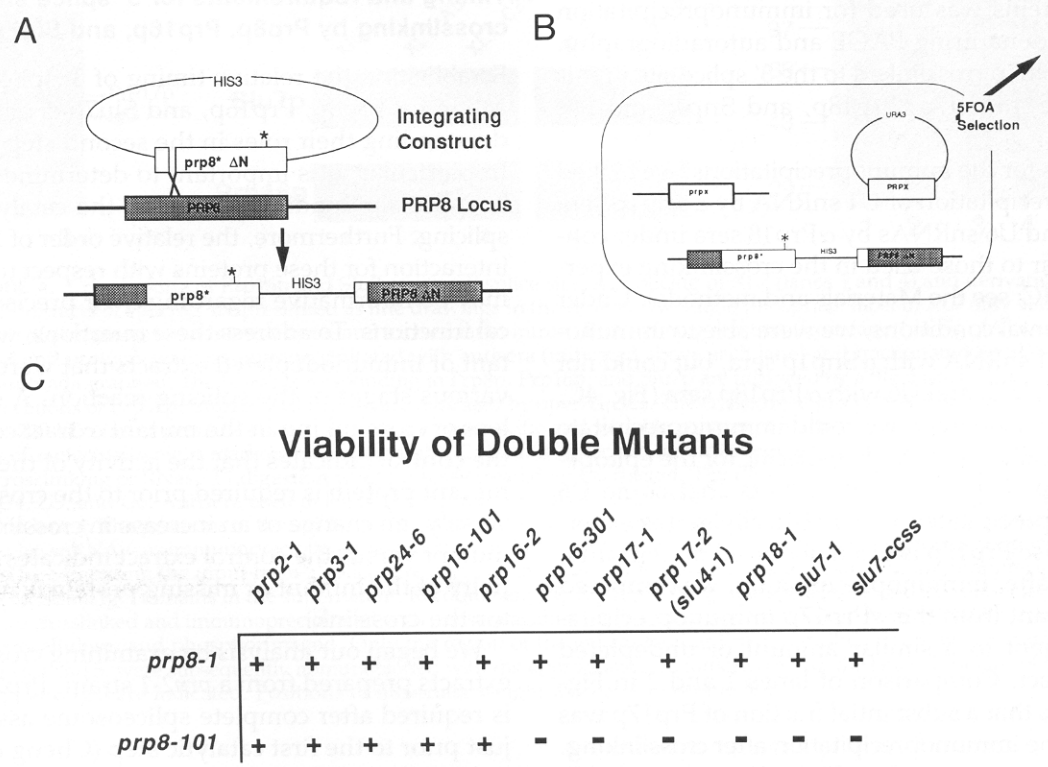

FIGURE 3. Genetic interactions between *prp8-101* and second step mutants. **A:** A gapped, integrating, *HIS3*-marked plasmid containing an N-terminally truncated copy of *prp8-1* or *prp8-101* (open box) is shown recombining with the chromosomal *PRP8* locus (shaded box). The mutation is indicated by a * symbol. The integration produces one full-length copy of *prp8-1* or *prp8-101* and an N-terminally truncated, nonfunctional copy of *PRP8, PRP8*ΔN. **B:** The *prp8* mutants from A were introduced directly into cells containing a second *prp* mutation (*prpx*) that is complemented by a wild-type (*PRPX*), *URA3*-marked plasmid. Selection on 5FOA generates a *prp8-1 prpx* or *prp8-101 prpx* double mutant strain (see the Materials and methods for details). **C:** A + symbol indicates that the double-mutant combination is viable and a − indicates that the double-mutant combination is inviable and that the two mutations are synthetically lethal.

allele (*prp16-301*), but not with a temperature-sensitive allele (*prp16-2*) or a mutant branch site suppressor (*prp16-101*). In contrast, *prp8-1* showed no genetic interactions with the *prp* mutants we tested. Prp8p, therefore, appears to function coordinately with the other second step splicing proteins.

Crosslinking of Prp16p and Slu7p to the 3′ splice site

To test whether second step proteins other than Prp8p might function in 3′ splice site recognition, we determined whether any can be crosslinked to the 3′ splice site. Prp16p and Slu7p are particularly attractive candidates because their sequences and/or biochemical properties predict that they interact with spliceosomal RNAs (Schwer & Guthrie, 1991; Frank & Guthrie, 1992). Moreover, Slu7p is known to participate in 3′ splice site selection (Frank & Guthrie, 1992). We utilized our previously characterized XL7 substrate and crosslinking assay (Fig. 1B) to determine whether Prp16p, Slu7p, Prp17p, or Prp18p crosslink to the 3′ splice site. We also tested the U1 70K protein (Snp1p) as a control for a splicing factor most likely involved in the first step of splicing. After splicing and crosslinking in a wild-type extract, antisera raised against each of these proteins was used for immunoprecipitation followed by denaturing PAGE and autoradiography. Prp16p and Slu7p crosslinked to the 3′ splice site in this assay, whereas Prp17p, Prp18p, and Snp1p did not (Fig. 4B).

As controls for the immunoprecipitations, we looked at immunoprecipitation of U1 snRNA by αSnp1p sera or U4, U5, and U6 snRNAs by αPrp18 sera under conditions similar to those used in the crosslinking experiments (Fig. 4C; see the Materials and methods). Under our experimental conditions, we were able to immunoprecipitate U1 snRNA with αSnp1p sera, but could not precipitate U4, U5, and U6 with αPrp18p sera (Fig. 4C, lanes 2 and 3). However, we could immunoprecipitate U4, U5, and U6 with antibodies specific for the epitope-tagged Prp8p (Fig. 4C, lane 1). Note that some U6 snRNA also precipitated nonspecifically in this experiment. Because Prp17p is often obscured on immunoblots by IgG after immunoprecipitation, we compared the supernatant from the αPrp17p immunoprecipitation experiment to a similar amount of undepleted splicing extract. Comparison of lanes 1 and 2 in Figure 4D shows that a substantial fraction of Prp17p was depleted in the immunoprecipitation after crosslinking. In summary, these controls indicate that only a specific subset of splicing factors crosslink to the 3′ splice site.

To determine whether Prp16p and Slu7p crosslink to the 3′ splice site in active spliceosomes, we employed two derivatives of XL7, XL7-A5 and XL7-C259 (Umen & Guthrie, 1995). XL7-A5 contains a G to A mutation at the fifth position of the intron and undergoes no splicing. We see no 3′ splice site crosslinking to either Prp16p or Slu7p with this substrate (Fig. 4A,E, lane 1 versus 2). XL7-C259 contains an A to C mutation at the branch residue and splices 5–10-fold less efficiently than XL7 (Fig. 4A, lane 1 versus 3). Similarly, Prp16p and Slu7p show a 5–10-fold decrease in 3′ splice site crosslinking with XL7-C259 (Fig. 4E, lane 1 versus 3). These results indicate that Prp16p and Slu7p crosslink to the 3′ splice site in active spliceosomes.

To ascertain whether the Prp16p and Slu7p crosslinks were specific to the 3′ splice site, we used a modified crosslinking substrate (XL7-E2). In XL7-E2, the second exon is uniformly labeled beginning nine nucleotides downstream of the 3′ splice junction and is substituted with 5-bromo-uridine (Umen & Guthrie, 1995). Both of these proteins failed to crosslink to XL7-E2 (Fig. 4A, lane 5; Fig. 4E, lanes 4 and 5). Immunoblotting of the samples indicated that the crosslinked protein in each immunoprecipitate co-migrates with the signal from the immunoblot (data not shown), and that similar amounts of protein were immunoprecipitated in each sample (Fig. 4F, lane 1 versus 2 and lane 3 versus 4). Therefore, Prp16p and Slu7p interact specifically with the 3′ splice site.

Timing and requirements for 3′ splice site crosslinking by Prp8p, Prp16p, and Slu7p

Establishing the relative timing of 3′ splice site interaction for Prp8p, Prp16p, and Slu7p is critical for understanding their roles in the second step of splicing. In particular, it is important to determine the time of 3′ splice site binding relative to the catalytic steps of splicing. Furthermore, the relative order of 3′ splice site interaction for these proteins with respect to each other may be informative regarding their precise biochemical functions. To address these questions, we used mutant or immunodepleted extracts that were blocked at various stages of the splicing reaction. A decrease or loss of crosslinking in the mutant extract compared to the control indicates that the activity of the missing or mutant protein is required prior to the crosslink. Conversely, no change or an increase in crosslinking in the mutant versus the control extract indicates that the activity of the mutant or missing protein is not required for the crosslink.

We began our analysis by examining crosslinking in extracts prepared from a *prp2-1* strain. Prp2p function is required after complete spliceosome assembly and just prior to the first catalytic step (Cheng & Abelson, 1987; Kim & Lin, 1993). Because the *prp2-1*-encoded protein is thermolabile in vitro, we compared crosslinking of Prp8p, Prp16p, and Slu7p in *prp2-1* extracts with and without heat inactivation. These extracts were fully complementable with purified Prp2p (data not shown). We found that crosslinking is abolished for all three proteins when spliceosomes are blocked at the Prp2p

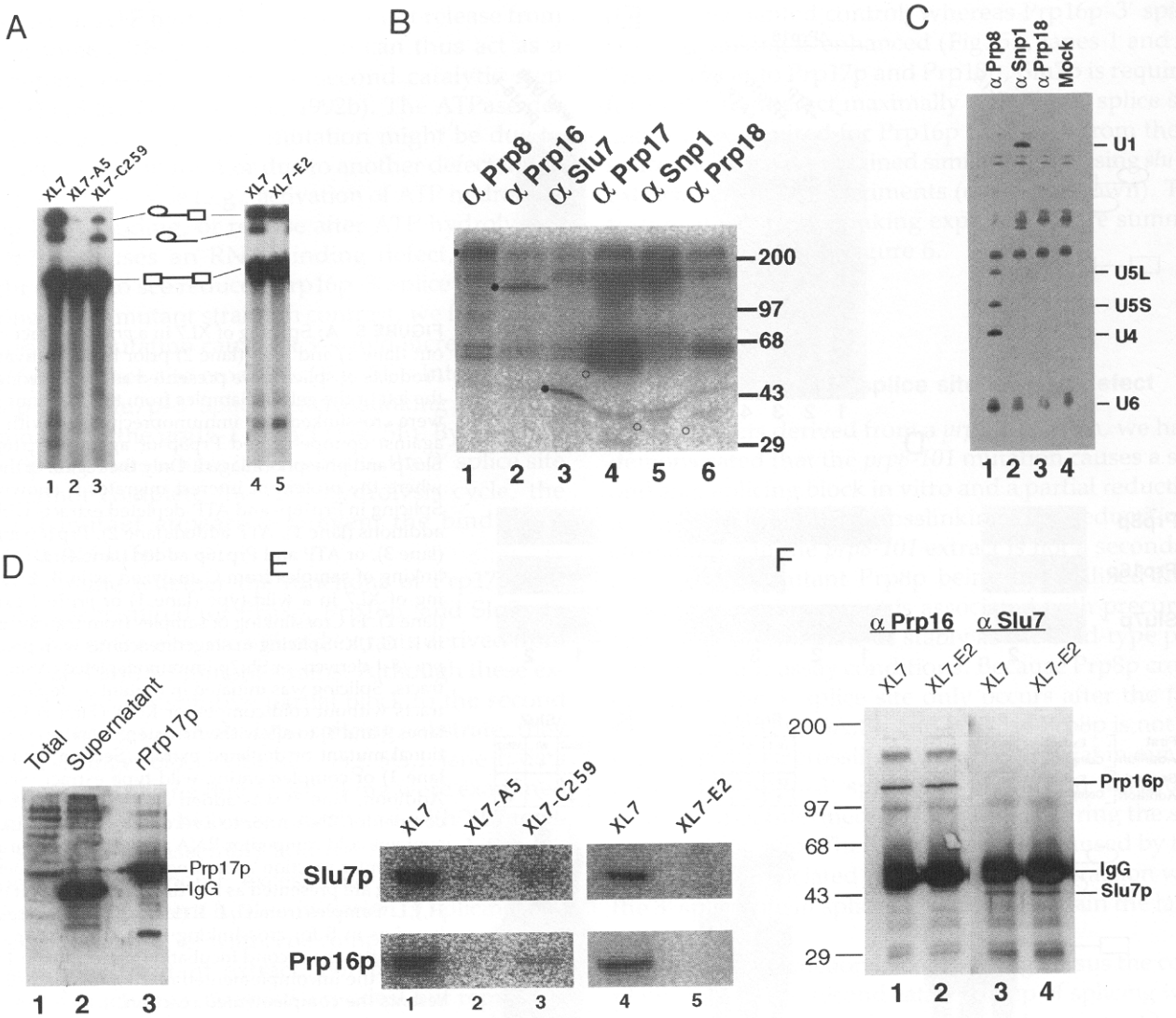

FIGURE 4. Crosslinking of Prp16p and Slu7p to the 3′ splice site. **A:** Splicing of XL7 (lanes 1 and 4) and derivatives (see text). Products of splicing are presented as line drawings in the center. The single phosphate label in XL7 only allows detection of precursor, lariat intermediate, and excised lariat intron. **B:** A splicing reaction (from lane 1 in Fig. 4A) was crosslinked and proteins were immunoprecipitated with antisera (indicated above each lane) and fractionated by SDS-PAGE and autoradiographed. The bands corresponding to Prp8p, Prp16p, and Slu7p are indicated by a filled circle. The presumptive locations of Prp17p, Snp1p, and Prp18p are indicated by open circles. The crosslinked proteins at ~66 kDa, ~150 kDa, and ~220 kDa (most prominent in lanes 4–6) are nonspecific and variable contaminants in immunoprecipitations. Positions of molecular weight markers are on the right. **C:** Immunoprecipitation reactions similar to those in B, except without crosslinking or RNase T1 digestion were protease treated and extracted. The RNAs were fractionated and probed for U1, U4, U5, and U6. Antisera used in lanes 1–3 are indicated above each lane and compared to a mock reaction (no antisera) in lane 4. The positions of the snRNAs are indicated. Bands not corresponding to these are nonspecific contaminants. Some U6 snRNA was immunoprecipitated nonspecifically in this experiment. **D:** Immunoprecipitation of Prp17p was evaluated by comparing the input from a splicing reaction as in B (lane 1) to the supernatant from the immunoprecipitation (lane 2). Some IgG remains in the supernatant. Recombinant Prp17p (lane 3) was used as a size standard. **E:** Samples from A were crosslinked and immunoprecipitated with antisera against Slu7p or Prp16p, fractionated by SDS-PAGE, transferred to nitrocellulose, and phosphorimaged. Only the region of the gel containing Prp16p or Slu7p is shown. **F:** Samples in E, lanes 4 and 5, were subsequently immunoblotted with the appropriate sera indicated above the lanes. Positions of Prp16p, Slu7p, and IgG are indicated. Positions of molecular weight markers are on the left.

step (Fig. 5A,B). Thus, crosslinking appears to occur either immediately prior to or after the first catalytic step of splicing.

Next, we examined the Prp16p-dependent step of splicing. Spliceosomes were formed in extract that had been immunodepleted for Prp16p, and then glucose and hexokinase were added to deplete ATP. We added either buffer, ATP, purified Prp16p, or both purified Prp16p and ATP to these spliceosomes and continued the incubation to allow completion of splicing. Splicing and crosslinking were then examined in each sample. As reported previously, the splicing reaction can only

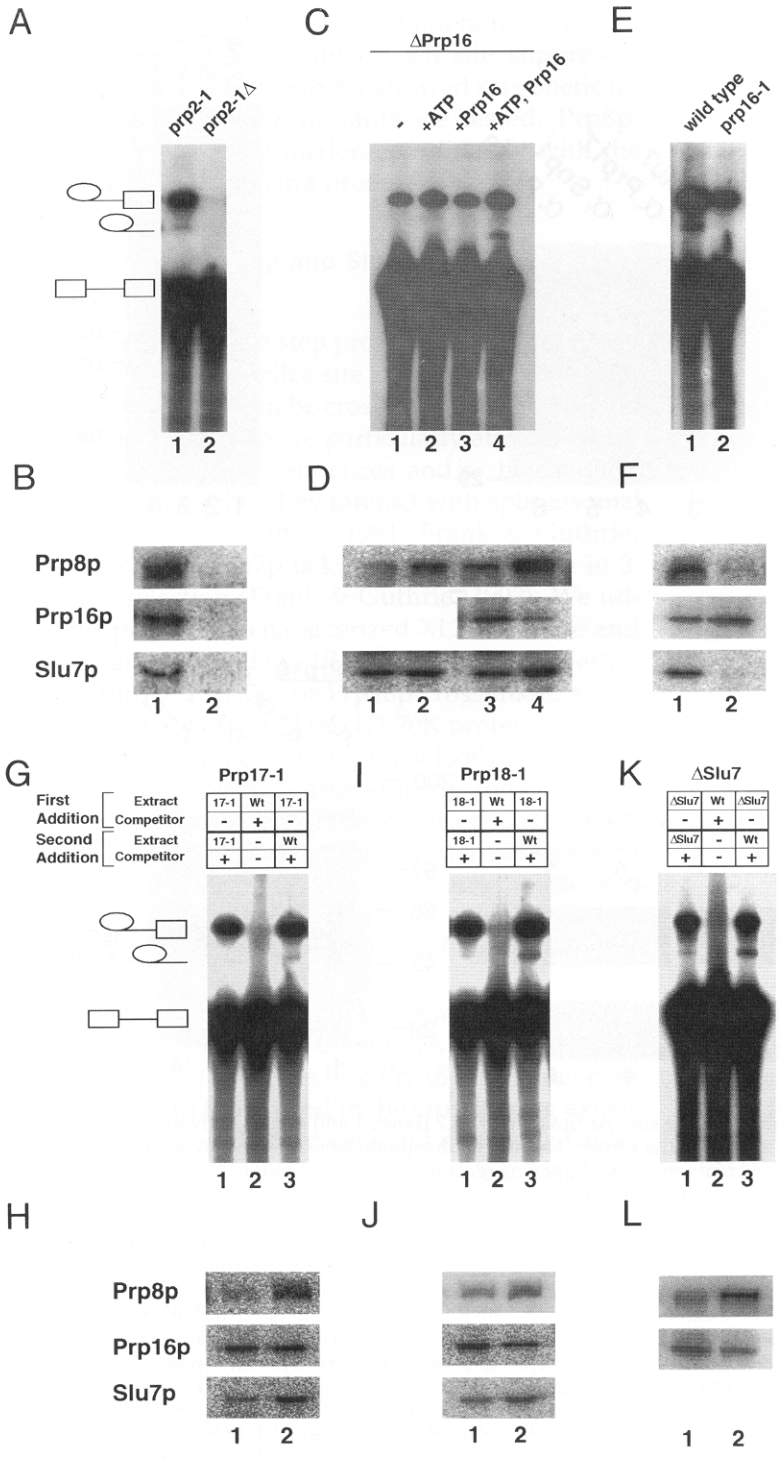

FIGURE 5. **A:** Splicing of XL7 in a *prp2-1* extract without (lane 1) and with (lane 2) prior heat inactivation. Products of splicing are presented as line drawings to the left of the gel. **B:** Samples from the reactions in A were crosslinked and immunoprecipitated with sera against epitope-tagged Prp8p or against Prp16p or Slu7p and phosphorimaged. Only the region of the gel where the protein of interest migrates is shown. **C:** Splicing in Prp16p- and ATP-depleted extracts with no additions (lane 1), ATP added (lane 2), Prp16p added (lane 3), or ATP and Prp16p added (lane 4). **D:** Crosslinking of samples from C analyzed as in B. **E:** Splicing of XL7 in a wild-type (lane 1) or *prp16-1* extract (lane 2). **F:** Crosslinking of samples from E analyzed as in B. **G,I,K:** Splicing in staged reactions with *prp17-1*, *prp-18-1*-derived, or Slu7p-immunodepleted (ΔSlu7) extracts. Splicing was initiated in mutant or depleted extracts without cold competitor RNA (First Addition, lanes 1 and 3) to allow the first step of splicing. Additional mutant or depleted extract (Second Addition, lane 1) or complementing wild-type extract (Second Addition, lane 3) was added along with excess cold competitor RNA prior to a second incubation. Lane 2 contains cold competitor RNA added at the beginning of a similar reaction as in lanes 1 and 3. Products of splicing are presented as line drawings to the left of G. **H,J,L:** Samples from G, I, K (lanes 1 and 3) were analyzed as in B for crosslinking to Prp8p, Prp16p, and Slu7p after the second incubation period. Lane 1 represents the uncomplemented reaction and lane 2 represents the complemented reaction.

be complemented with the addition of both ATP and Prp16p (Fig. 5C) (Schwer & Guthrie, 1991). Furthermore, Prp8p and Slu7p crosslink to the 3′ splice site in the absence of Prp16p, but require hydrolysis of ATP by Prp16p for maximal crosslinking (Fig. 5D, lanes 1–3 versus lane 4). We consistently observe a 2–3-fold increase in Prp8p and Slu7p crosslinking to the 3′ splice site when the reaction is complemented with Prp16p and ATP. In contrast, Prp16p crosslinks to the 3′ splice site 2–3-fold more strongly in the absence of ATP than in its presence, consistent with its release from spliceosomes upon ATP hydrolysis (Fig. 5D, lane 3 versus 4) (Schwer & Guthrie, 1991). The slowed reaction kinetics of the splicing substrate XL7 most likely account for the remaining Prp16p in spliceosomes after complementation.

We also examined crosslinking in an extract derived from a *prp16-1* strain. The protein encoded by the *prp16-1* allele can bind spliceosomes, but is strongly

reduced for ATP hydrolysis and does not release from spliceosomes. The mutant protein can thus act as a "dominant negative" for the second catalytic step (Fig. 5E) (Schwer & Guthrie, 1992b). The ATPase defect caused by the *prp16-1* mutation might be due to poor binding of an RNA or due to another defect in the ATP hydrolysis cycle (e.g., activation of ATP hydrolysis upon RNA binding, or release after ATP hydrolysis). If *prp16-1* causes an RNA binding defect, then we might expect to see reduced Prp16p–3′ splice site crosslinking in the mutant strain. In contrast, we found that the *prp16-1* mutation caused a 3–4-fold increase in the Prp16p–3′ splice site crosslink (Fig. 5F). Interestingly Prp8p- and Slu7p–3′ splice site crosslinking are nearly eliminated in the *prp16-1* extract (Fig. 5F). By trapping Prp16p in a state where it is bound to the 3′ splice site but cannot complete the ATP hydrolysis cycle, the *prp16-1* mutant appears to prevent the binding of Prp8p and Slu7p.

To examine whether the functions of Prp17p and Prp18p are required for Prp8p, Prp16p, and Slu7p to bind the 3′ splice site, we utilized extracts derived from *prp17-1* and *prp18-1* mutant strains. Although these extracts cause a constitutive partial block to the second step of splicing for a wild-type splicing substrate, they cause a stronger block with XL7 (Fig. 5G,I, lane 1; data not shown). Splicing and crosslinking were examined in these extracts, which were incubated with XL7 to allow spliceosome assembly and the first catalytic step to occur. At this point, excess cold competitor RNA was added to prevent further initiation of splicing, followed by a "chase" of wild-type complementing extract or additional mutant extract. For both *prp17-1* and *prp18-1* extracts, we observed a modest but reproducible increase in Prp8p- and Slu7p–3′ splice site crosslinking when the defect was complemented (Fig. 5H,J, lanes 1 and 2). In contrast, the Prp16p–3′ splice crosslink stays the same or is diminished slightly upon complementation. Thus, although Prp17p and Prp18p are required for Prp8p and Slu7p to crosslink maximally to the 3′ splice site, their functions are not required for the Prp16p–3′ splice site interaction. Moreover, Prp18p may facilitate the release of Prp16p from spliceosomes because there is usually greater Prp16p crosslinking in the mutant versus complemented reaction (Fig. 5J, lanes 1 and 2).

Finally, we determined whether Prp8p or Prp16p require Slu7p to bind the 3′ splice site. We followed a similar protocol as described for *prp17-1* and *prp18-1* extracts, except we utilized an extract that had been immunodepleted with αSlu7p sera (ΔSlu7). XL7 was incubated in this extract, and splicing and 3′ splice site crosslinking were examined. The extent of Slu7p immunodepletion is variable, and in this experiment, caused only a partial second step splicing block (Fig. 5K, lane 1 versus lane 3). In ΔSlu7 extracts, Prp8p–3′ splice site crosslinking is consistently reduced compared to the complemented control, whereas Prp16p–3′ splice site crosslinking is enhanced (Fig. 5L, lanes 1 and 2). Thus, similar to Prp17p and Prp18p, Slu7p is required for Prp8p to interact maximally with the 3′ splice site and is also required for Prp16p to release from the 3′ splice site. We have obtained similar results using *slu7-1* extracts for these experiments (data not shown). The results of these crosslinking experiments are summarized in Table 1 and Figure 6.

DISCUSSION

prp8-101 causes a 3′ splice site binding defect

Using extracts derived from a *prp8-101* strain, we have demonstrated that the *prp8-101* mutation causes a second step splicing block in vitro and a partial reduction in Prp8p–3′ splice site crosslinking. The reduction in crosslinking in the *prp8-101* extract is not a secondary result of the mutant Prp8p being destabilized from spliceosomes, because it is associated with precursor and lariat intermediate as stably as the wild-type protein under our assay conditions. Because Prp8p crosslinking to the 3′ splice site only occurs after the first catalytic step (Fig. 5A,B), and because Prp8p is not associated with or crosslinked to excised lariat in our extracts, the Prp8p–3′ splice site interaction must take place in lariat intermediates prior to or during the second catalytic step. Therefore, the defect caused by this mutation is associated with a reduced interaction with the 3′ splice site in spliceosomes that contain the lariat intermediate.

The partial reduction in crosslinking versus the complete block to the second catalytic step of splicing with this mutant has several possible explanations. One is that a minimal occupancy time by Prp8p at the 3′ splice

TABLE 1. Summary of 3′ splice site crosslinking to Prp8p, Prp16p, and Slu7p.[a]

Extract	Prp8 x-link	Prp16 x-link	Slu7 x-link
Wild-type	+	+	+
prp8-101	+/−	n.d.	n.d.
prp2-1	−	−	−
ΔPrp16	+/−	n.a.	+/−
ΔPrp16 + ATP	+/−	n.a.	+/−
ΔPrp16 + 16	+/−	++	+/−
ΔPrp16 + ATP + 16	+	+	+
prp16-1	−	++	−
Prp17-1	+/−	+	+/−
Prp18-1	+/−	++	+/−
ΔSlu7	+/−	++	n.a.

[a] 3′ splice site crosslinking to Prp8p, Prp16p, and Slu7p in mutant or depleted extracts is expressed in comparison to a wild-type or control (complemented) extract; +, wild-type levels of crosslinking; +/−, less than wild-type levels of crosslinking; −, no detectable crosslinking; ++, greater than wild-type levels of crosslinking; n.d., experiment not done; n.a., not applicable.

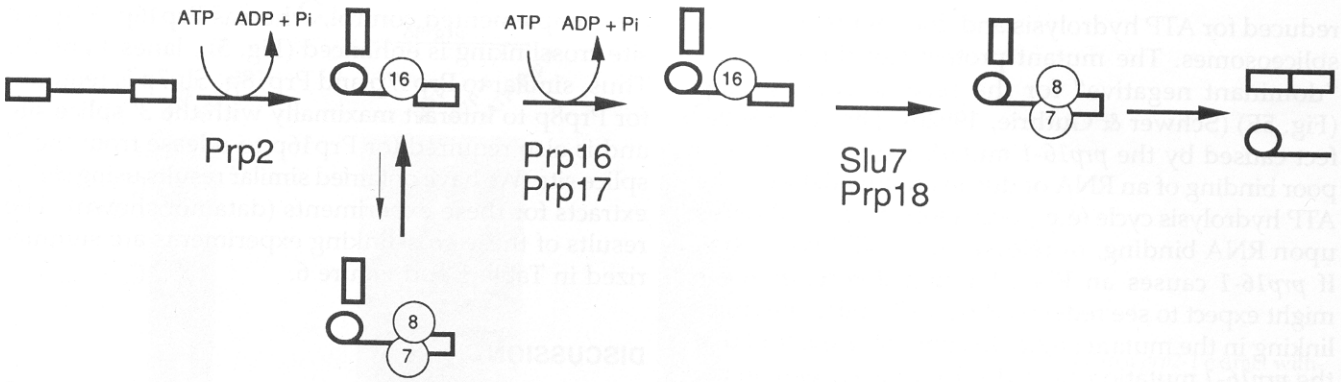

FIGURE 6. Model for ordered interactions of Prp8p, Prp16p, and Slu7p with the 3′ splice site. A line drawing summary of a splicing reaction starting with the Prp2p-dependent step and indicating gene product and ATP hydrolysis requirements. Proteins bound to the 3′ splice site are indicated by the spheres labeled 16 (Prp16p), 7 (Slu7p), and 8 (Prp8p). After the Prp2p step, Prp16p binds strongly to the 3′ splice site and Slu7p and Prp8p can bind weakly. After hydrolysis of ATP by Prp16p, and the Prp17p-, Prp18p-, and Slu7p-dependent steps, Prp8p and Slu7p bind maximally to the 3′ splice site. Prp17p is shown acting at the Prp16p-dependent step because Prp17p is known to function at or before an ATP requiring step (Jones et al., 1995), but is not necessary for Prp16p to bind the 3′ splice site. Slu7p and Prp18p function in a ATP-independent manner and are placed after the Prp16p- and Prp17p-requiring steps (Horowitz & Abelson, 1993a; Athar & Schwer, 1995; Jones et al., 1995). Prp8p is at the 3′ splice site just prior to (and possibly during) catalysis and leaves the 3′ splice site afterward. The same is presumed to be true of Slu7p.

site is required for catalysis and the *prp8-101* mutation reduces binding below that minimum, but does not eliminate binding. It is important to bear in mind that crosslinking represents an interaction between two molecules but is not a direct measure of binding. It can overrepresent binding-site occupancy of a protein because it permanently "captures" binding events in a given interval of time. Thus, the apparent modest binding defect caused by the *prp8-101* mutation may be more severe than it appears from crosslinking. This also applies to the crosslinking results we obtain for Prp8p, Prp16p, and Slu7p in mutant or depleted extracts (Fig. 5). The modest but reproducible changes in 3′ splice site crosslinking for Prp16p, Prp8p, and Slu7p may represent more severe alterations in 3′ splice site binding than is apparent from differences in crosslinking efficiency. A second explanation for the small reduction in Prp8p–3′ splice crosslinking in *prp8-101* extracts is that reduced binding might cause only part of the splicing defect. For example, the block to splicing could involve a loss of communication between Prp8p and another splicing component that activates 3′ splice site usage (see below), or could be due to binding in an altered conformation. These issues can be addressed more readily when a direct assay for 3′ splice site binding is developed. We are also currently mapping the domain(s) of Prp8p that is required for its 3′ splice site interaction.

prp8-101 interacts genetically with second step mutants

By constructing double mutant strains, we have shown synthetic lethal interactions between *prp8-101* and alleles of *PRP16*, *PRP17*, *PRP18*, and *SLU7*, but not with alleles of first step splicing mutants. That a more severe allele of *PRP8*, *prp8-1*, does not show genetic interactions with the second step splicing mutants demonstrates the sensitivity and selectivity of this assay. Furthermore, among the second step splicing mutants there is some specificity; *prp8-101* is only synthetically lethal with a cold-sensitive allele of *PRP16* (*prp16-301*) and not a temperature-sensitive allele (*prp16-2*) or a branch site suppressor allele (*prp16-101*). We have also tested a *prp16-1 prp8-101* double mutant and found a strong synthetic growth defect, but not synthetic lethality (data not shown). *prp16-1* is similar to *prp16-101* in its ability to suppress mutant branch sites, and to *prp16-301*, in its cold sensitive, dominant negative phenotype. However, the phenotype of *prp16-1* is not as severe as that of *prp16-301*. Because *prp16-101* suppresses branch site mutations as well or better than *prp16-1* (Burgess & Guthrie, 1993), branch site suppression per se is not the basis for the genetic interaction we see between *prp16-1* and *prp8-101*. Instead, the severity of the genetic interactions between *prp16-1* or *prp16-301* and *prp8-101* correlates with the severity of the cold-sensitive, dominant negative phenotypes caused by the *prp16* alleles. These phenotypes appear to stem from the nonproductive binding of mutant Prp16p to spliceosomes (Schwer & Guthrie, 1992b; Madhani & Guthrie, 1994b). *prp16-1* inhibits the association of Prp8p with the 3′ splice site and the same is likely to be true of *prp16-301*. The other genetic interactions between *prp8-101* and second step mutants might also be explained by the biochemical phenotypes we observe. Individually, each of these mutants impairs binding of Prp8p to the 3′ splice site. When com-

bined with *prp8-101*, binding might be eliminated and thus cause a severe block to the second step of splicing in vivo.

Another explanation for the genetic interactions between *prp8-101* and the other second step splicing mutants is that the proteins they encode are physically associated in a complex that is only partly disrupted by individual mutant alleles, but is rendered nonfunctional with two mutant subunits. Although immunodepletion and complementation experiments argue against a stable extra-spliceosomal complex that contains these proteins (Schwer & Guthrie, 1991; Horowitz & Abelson, 1993a; Athar & Schwer, 1995; Jones et al., 1995), they may associate only on the spliceosome. Because Prp8p is an integral and highly conserved spliceosomal protein (Anderson et al., 1989; Pinto & Steitz, 1989; Hodges et al., 1995), it is a good candidate for forming part of a spliceosomal binding site for the exchangeable second step factors. Whether or not they function as a complex, it is clear from the 3′ splice site binding studies above that there is a great deal of functional interdependence among the second step splicing factors.

The 3′ splice site is recognized in two distinct steps

Although both Prp16p and Slu7p are predicted to be RNA binding proteins, Prp16p associates with spliceosomes only transiently and the same is likely to be true of Slu7p (Schwer & Guthrie, 1991; D. Frank, unpubl. obs.). Furthermore, their affinities for spliceosomal RNAs are probably highly regulated and binding may require a very specific conformation of spliceosomal RNAs and proteins that would be difficult to reproduce with purified proteins and RNA. As an alternative strategy, site-specific UV crosslinking with a kinetically slowed substrate has allowed us to identify specific interactions between the 3′ splice site and Prp16p and Slu7p in active spliceosomes.

Using splicing extracts that are blocked at specific steps of the reaction, we determined when Prp8p, Prp16p, and Slu7p interact with the 3′ splice site. With an extract blocked at the Prp2p-requiring step of splicing, we established that the 3′ splice site interaction of these proteins takes place immediately prior to or, most likely, after the first catalytic step. This finding is important because it establishes a correlation between the time of 3′ splice site interaction for Prp8p, Prp16p, and Slu7p and the time in the splicing reaction when they are functionally required. This result has also been seen for Prp8p using site-specific 4-thio-uridine crosslinking at the 3′ splice site (Teigelkamp et al., 1995a).

We have also shown that Prp16p interacts with the 3′ splice site after the first catalytic step and prior to its hydrolysis of ATP. Although Prp8p and Slu7p can crosslink to the 3′ splice site prior to Prp16p binding to the spliceosome, they require hydrolysis of ATP by Prp16p for maximal interaction with the 3′ splice site. It is possible that the weaker 3′ splice crosslinking of Prp8p and Slu7p in the absence of Prp16p and ATP is due to incomplete removal of Prp16p by immunodepletion. However, we also observe residual binding of Prp8p to the 3′ splice site in heat-inactivated extracts prepared from a thermolabile mutant strain, *prp16-2* (data not shown). Because this experiment involves a completely independent means of removing Prp16p activity, the weaker 3′ splice site interaction we observe for Prp8p and Slu7p in ΔPrp16 extracts is unlikely to be artifactual. This result is interesting in light of the observation that, in *prp16-1*-derived extracts, in which the mutant Prp16p binds tightly to spliceosomes (Schwer & Guthrie, 1992b), crosslinking of Prp8p and Slu7p is largely precluded. It appears from this result that the Prp16p–3′ splice site interaction is mutually exclusive with the 3′ splice site interactions of Prp8p and Slu7p. In contrast, purified wild-type Prp16p added to ΔPrp16 spliceosomes in the absence of ATP does not seem to affect the 3′ splice site interaction of Prp8p and Slu7p. Therefore, wild-type Prp16p must either be more exchangeable than the *prp16-1*-encoded protein (Schwer & Guthrie, 1992b) or must bind in a conformation that does allow Prp8p and Slu7p to interact with the 3′ splice site.

These results establish that the 3′ splice site interaction of Prp16p and ATP hydrolysis by Prp16p precede a strong 3′ splice site interaction with Prp8p and Slu7p. The weaker interaction with the 3′ splice site by Prp8p and Slu7p in the absence of Prp16p may represent a 3′ splice site proofreading or inspection step that is required prior to the conformational change induced when Prp16p hydrolyzes ATP. Interestingly, Prp16p, Slu7p, and Prp8p can interact with the 3′ splice site prior to ATP hydrolysis by Prp16p, but do not confer protection to the 3′ splice site from oligonucleotide directed RNase H cleavage (Schwer & Guthrie, 1992a). After ATP hydrolysis by Prp16p, either additional factors must bind the 3′ splice site and/or Prp8p and Slu7p must bind in a manner that allows increased protection.

The transition from weak to strong 3′ splice site binding by Prp8p and Slu7p might correspond to the LI → LI* transition proposed by Burgess and Guthrie (1993) as a key step in a kinetic pathway for maintaining fidelity of intron recognition. Both Prp8p and Slu7p are known to affect 3′ splice site selection (Frank & Guthrie, 1992; Umen & Guthrie, 1995) and might need to "examine" a potential 3′ splice site in a low-affinity binding mode before a decision is made regarding that splice site's utilization. This would explain the apparent lack of sequence specificity seen in experiments where Prp8p can be crosslinked to 4-thio-uridine at nonutilized 3′ splice sites (Teigelkamp et al., 1995a). Although crosslinking to a position that is formally +13 in the second exon was observed, this crosslink is in a region

of the substrate that *can* be utilized as a 3′ splice acceptor when there is no upstream 3′ splice site. In contrast, we see no Prp8p crosslinking to positions downstream of +9 in the second exon of XL7 (Umen & Guthrie, 1995) and, correspondingly, this region of the substrate is never used as a 3′ splice acceptor in vitro or in vivo (J.G. Umen & C. Guthrie, unpubl. obs.). It is also possible that the discrepancy we see is due to the exons of different splicing substrates having differing affinities for Prp8p.

Our results with *prp17* and *prp18* mutant extracts and ΔSlu7 immunodepleted extracts are consistent with Prp17p, Prp18p, and Slu7p being required for strong interaction of Prp8p with the 3′ splice site and with Prp17p and Prp18p being required for strong interaction of Slu7p with the 3′ splice site. Furthermore, it appears that release of Prp16p from the 3′ splice site is dependent on Slu7p and also possibly Prp18p. This requirement cannot be absolute for Prp18p because this protein is not essential for splicing in vitro or in vivo (Horowitz & Abelson, 1993a, 1993b). Notably, both Slu7p and Prp18p act at an ATP-independent step of splicing (Horowitz & Abelson, 1993a; Athar & Schwer, 1995; Jones et al., 1995), which formally places their functions "downstream" of the Prp16p-dependent step. However, it is clear that there exists an interdependent relationship between Slu7p and Prp16p: Prp16p requires Slu7p for 3′ splice site release and Slu7p requires Prp16p to interact strongly with the 3′ splice site. This mutual dependence might serve to couple the functions of the two proteins and enhance the fidelity or specificity of 3′ splice site selection.

In summary, Prp16p crosslinking to the 3′ splice site occurs after the first catalytic step of splicing and is independent of ATP binding or hydrolysis. Maximal 3′ splice site crosslinking by Prp8p and Slu7p occurs after Prp16p hydrolyzes ATP and, presumably, after it exits the spliceosome. Thus, the 3′ splice site is recognized in two distinct steps (see Fig. 6). This result is consistent with experiments in mammalian extracts that also suggest at least two separate 3′ splice site recognition events (Reed, 1989; Zhuang & Weiner, 1990). However, unlike yeast, many mammalian introns require the 3′ splice site to initiate spliceosome assembly and at least one of the mammalian 3′ splice site recognition events is likely to occur prior to the first catalytic step (Reed & Maniatis, 1985; Ruskin & Green, 1985; Rymond & Rosbash, 1985; Lamond et al., 1987; Rymond et al., 1987). In contrast, the 3′ splice site recognition events we have analyzed occur exclusively during the second catalytic step. Furthermore, the 3′ splice site crosslinking interactions of Prp8p and Slu7p define at least one additional event that occurs after both the ATP-dependent stage of the second catalytic step (defined by Prp16p and Prp17p) and the ATP-independent stage (defined by Slu7p and Prp18p), but before catalysis. We cannot yet distinguish whether Prp8p and Slu7p crosslink to the 3′ splice site sequentially or simultaneously. In either case, Prp8p and Slu7p bind the 3′ splice site at the closest interval to catalysis that can presently be identified (Fig. 6).

Although catalysis in pre-mRNA splicing is thought to be mediated primarily by snRNAs, this does not rule out participation by protein factors. Because Prp8p is, to date, the most evolutionarily conserved protein in the spliceosome (Anderson et al., 1989; Pinto & Steitz, 1989; Hodges et al., 1995), it is a good candidate for being involved in the catalytic steps of the reaction. Our results strengthen this hypothesis by establishing the presence of Prp8p at or near the active site just prior to and/or during the second catalytic step of the reaction.

MATERIALS AND METHODS

Strains

Yeast strains are listed in Table 2. *Escherichia coli* strain DH5α was used as a recipient for all cloning procedures described.

Genetic methods

Standard yeast genetic methods were used for the manipulations described here (Guthrie & Fink, 1991). For double mutant analysis, plasmids pJU190 (*prp8-101*) or pJU213 (*prp8-1*) were cut with *Hpa* I and transformed into recipient yeast strains carrying a *prp* mutation (either chromosomally or on a single-copy plasmid complementing a chromosomal deletion) and a URA3-marked plasmid with a wild-type copy of the mutant *PRP* gene. For pJU190, 40–60% of His+ transformants displayed the *prp8-101* phenotype (cold sensitivity, altered 3′ splice site usage) and for pJU213, 80–90% of His+ transformants displayed a *prp8-1* phenotype (temperature sensitivity). Approximately 60 individual transformants were examined for each experiment. These transformants were replica plated to 5FOA-containing plates and scored for viability. Because the integration frequency of *prp8-101* with pJU190 is ~50%, this frequency of $5FOA^-$ tranformants is indicative of synthetic lethality. For pJU190, either ~50% of the transformants did not grow on 5FOA, indicating synthetic lethality with the *prp* mutant being tested, or 98–100% grew on 5FOA, indicating no genetic interaction. For pJU213, 98–100% of the transformants always grew on 5FOA, indicating no genetic interactions with *prp* mutants that were tested. Double mutants were assayed at the permissive temperature of 25 °C.

Plasmids

Plasmid pJU204 (*PRP8-HA3*) has been described (Umen & Guthrie, 1995). pJU206 (*prp8-101-HA3*) was constructed from pJU204 by replacing the 1.9-kb *Cla* I fragment from pJU204 with the same fragment from a *prp8-101* clone. The *prp8-101*-integrating plasmid pJU190 was constructed by inserting a *Sal* I–*Nhe* I fragment from a YCP50 *prp8-101* clone into the *Sal* I and *Xba* I sites of the *HIS3* marked integrating plasmid RS303 (Sikorski & Hieter, 1989). The *prp8-1* version of this plasmid was constructed by PCR amplifying the 1.9-kb

TABLE 2. *S. cerevisiae* strains used in this study.

Name	Genotype	Reference
YJU76	Matα prp8Δ::LEU2 leu2-3 leu2-112 ura3-52 ade2-101 his3Δ1 trp1-289 prp4Δ::TRP1 pJU186 (PRP8-HIS3-CEN-ARS)	Umen and Guthrie (1995)
YJU77	YJU76 except contains plasmid pJU204 (PRP8-HA3) instead of pJU186	Umen and Guthrie (1995)
YJU78	YJU76 except contains plasmid pJU206 (prp8-101-HA3) instead of pJU186	This work
SS304	Matα prp2-1 ade2-1 his3-532 trp1-289 ura3-1 ura3-2	Lustig et al. (1986)
TR1-3	Matα his3 trp1 lys2-801 ura3-52 ade2-101 prp24Δ::LYS2 pYCpXba (PRP24-URA3-CEN-ARS)	Gift from Anita Jandrositz, University of California, San Francisco
SPJ3.33	Mat*a* prp3-1 his3 leu2 lys2 ura3-52	Lustig et al. (1986)
YDAF7-GK	Mat*a* ura3 lys2 his3 ade2 trp1 leu2 slu7Δ::TRP1 pYS7-7 (SLU7-URA3-CEN-ARS)	Frank and Guthrie (1992)
A7C8Aa	Mat*a* slu7-1 ura3-52 trp1-Δ63 his3-Δ200 leu2-Δ1 ade2-101 lys2-801	Frank and Guthrie (1992)
ts365	Mat*a* prp17-1 ade2-101 his3-Δ200 ura3-52 lys2-801	Vijayraghavan et al. (1989)
A4C15Ba	Mat*a* prp17-2 ura3-52 trp1-Δ63 his3-Δ200 leu2-Δ1 ade2-101 lys2-801	Frank et al. (1992)
ts503	Matα prp18-1 ade2-101 his3-Δ200 ura3-52 lys2-801	Vijayraghavan et al. (1989)
YS78	Mat*a* trp1 ura3 lys2 leu2 ade2 his3 prp16Δ::LYS2 pSB2 (PRP16-URA3-CEN-ARS)	Burgess and Guthrie (1993)

C-terminal *Cla* I fragment of *PRP8* from a *prp8-1* strain and then replacing the 1.9-kb *Cla* I fragment of pJU190 with the PCR-amplified *prp8-1* fragment. Plasmids for double-mutant analysis were from the following sources: *PRP2*, Chen and Lin (1990); *PRP3*, Last et al. (1987); *PRP24*, Shannon and Guthrie (1991); *prp24-6*, gift from Anita Jandrositz, University of California, San Francisco; *PRP17*, Jones et al. (1995); *PRP18*, Horowitz and Abelson (1993b); *SLU7* and *slu7-ccss*, Frank and Guthrie (1992); *PRP16*, *prp16-2*, *prp16-301*, and *prp16-101*, Burgess and Guthrie (1993).

Immunodepletions

Prp16p was removed from a wild-type extract containing epitope-tagged Prp8p (PRP8-HA3) by incubating 90 μL of extract with 18 μL (288 μg) protein A purified αPrp16p antibodies (Schwer & Guthrie, 1991) at 4 °C for 1 h. This reaction was added to 120 μL protein A sepharose beads in buffer D plus an additional 75 μL buffer D (Lin et al., 1985) and incubated at 4 °C for an additional hour with frequent agitation. After brief centrifugation, the supernatant was removed and used for splicing reactions. Slu7p was removed from extracts by a similar procedure, except that 80 μL of αSlu7p antibodies (960 μg) (Jones et al., 1995) were used and no additional buffer D was added.

Splicing, UV crosslinking, and immunoprecipitations

Splicing extracts were prepared as described previously (Umen & Guthrie, 1995). For mutant *prp* strains, an epitope-tagged version of *PRP8* (pJU204) was transformed into the strains prior to growth and extract preparation. Cells were grown in SD-His media to maintain selection for the plasmid until the last 2–3 generations. At this point they were transferred to YEPD, where they were grown until harvesting.

Splicing reactions were performed as described previously (Umen & Guthrie, 1995). When mutant extracts were complemented, they were first incubated for 20 min at 25 °C. A 300–500-fold molar excess of cold competitor RNA was then added with either a half reaction volume of wild-type complementing extract plus standard splicing salts or additional mutant extract plus standard splicing salts. The incubation was then continued for 10 min. For each experiment, an aliquot of the complementing extract mixture was removed before splicing commenced and mixed with cold competitor RNA as a control. The *prp2-1*-derived mutant extract was used with or without prior heat inactivation for 10 min at 37 °C. ΔPrp16 extracts were incubated for 20 min and then incubated at 30 °C for 10 min in the presence of 4 mM glucose and 8.5 units/mL of hexokinase (Boehringer). The reaction was then split into four parts that received either buffers only, 2.5 mM additional ATP and MgCl2, 2.5 pg/μL purified Prp16p in buffer D, or both ATP/MgCl2 and Prp16p. The incubation was then continued for 10 min at 25 °C.

UV crosslinking and immunoprecipitations were performed as described previously (Umen & Guthrie, 1995), except that 150 mM NaCl (instead of 300 mM KCl) was used in the wash buffers and no salt or NP40 were added to splicing reactions during incubation with antisera. Twelve micrograms αSlu7p antibodies or 8 μg αPrp16p antibodies (protein A purified) were used for immunoprecipitations from 40-μL reactions. αPrp17p (50 μL), αPrp18p (60 μL), and αSnp1p (80 μL) sera were pre-bound to protein A sepharose (40 μL) (Pharmacia) and incubated with crosslinking reactions (40 μL) in 500 μL NET150 (150 mM NaCl, 50 mM Tris, pH 7.4, 0.05% NP40) for 2 h at 4 °C prior to elution and SDS-PAGE. After electrophoresis, gels were transferred to nitrocellulose and autoradiographed or phosphorimaged. In some experiments, the nitrocellulose was then immunoblotted.

For denaturing immunoprecipitations, a splicing reaction containing epitope-tagged wild-type Prp8p was divided in half. One half was subject to UV crosslinking and the other was not. SDS was added to a final concentration of 5% and the samples were boiled for 3 min. Each sample was diluted 10-fold into NET150 that contained 1% Triton X-100, 1 μg 12CA5 antibody, 15 μL protein A sepharose, and protease inhibitors. After 1 h rocking at 4 °C, the beads were washed three times with NET150 and then treated with proteinase K and SDS. RNA was precipitated after phenol/chloroform extraction and fractionated on a 6% denaturing polyacrylamide gel.

snRNA immunoprecipitation controls (Fig. 3E) for Prp8p, Prp18p, and Snp1p involved mock splicing reactions that

were identical to normal reactions but did not contain XL7 or undergo UV crosslinking and RNase treatment. Pellets from the immunoprecipitate were proteinase K-treated and extracted and the RNA was precipitated and probed using oligos directed against U1, U4, U5, and U6 snRNAs (Bordonne et al., 1990).

The immunoprecipitation control for Prp17p was performed by TCA precipitating the supernatant from a crosslinking/immunoprecipitation experiment using 10% TCA. This was resuspended in protein sample buffer and compared to an equivalent amount of total starting extract before immunoprecipitation. These samples were fractionated by SDS-PAGE and immunoblotted to detect Prp17p. Some antibodies remain in the supernatant after immunoprecipitation, accounting for the signal beneath the Prp17p band on the gel in Figure 3D.

All immunoblotting was performed using an ECL kit from Amersham according to the manufacturer's instructions.

ACKNOWLEDGMENTS

We thank Liz Blackburn, Cathy Collins, Amy Kistler, Hiten Madhani, Chris Siebel, Peter Walter, and Yan Wang for comments on this manuscript. We thank Yan Wang for providing purified Prp16p and R.J. Lin for providing purified Prp2p. We thank Shelly Jones for providing αPrp17p sera and recombinant Prp17p, and Dan Frank for providing αSlu7p sera. We thank Paul Siliciano for providing αSnp1p sera and David Horowitz for providing αPrp18p sera. We are grateful for the excellent technical assistance of Heli Roiha, Carol Pudlow, and Lucita Esperas.

This work was supported by a NIH training grant and a NSF pre-doctoral fellowship to J.G.U., and NIH research grant GM21119 to C.G. C.G. is an American Cancer Society Research Professor of Molecular Genetics.

Received July 5, 1995; returned for revision July 25, 1995; revised manuscript received July 31, 1995

REFERENCES

Anderson GJ, Bach M, Luhrmann R, Beggs JD. 1989. Conservation between yeast and man of a protein associated with U5 small nuclear ribonucleoprotein. *Nature 342*:819–821.

Athar A, Schwer B. 1995. SLU7 and a novel activity, SSF1, act subsequent to PRP16 in the second step of yeast pre-mRNA splicing. *EMBO J*. Forthcoming.

Bordonne R, Banroques J, Abelson J, Guthrie C. 1990. Domains of yeast U4 spliceosomal RNA required for PRP4 protein binding, snRNP–snRNP interactions, and pre-mRNA splicing in vivo. *Genes & Dev 4*:1185–1196.

Brown JD, Beggs JD. 1992. Roles of PRP8 protein in the assembly of splicing complexes. *EMBO J 11*:3721–3729.

Burgess S, Couto JR, Guthrie C. 1990. A putative ATP binding protein influences the fidelity of branchpoint recognition in yeast splicing. *Cell 60*:705–717.

Burgess SM, Guthrie C. 1993. A mechanism to enhance mRNA splicing fidelity: The RNA-dependent ATPase Prp16 governs usage of a discard pathway for aberrant lariat intermediates. *Cell 73*:1377–1391.

Chen JH, Lin RJ. 1990. The yeast PRP2 protein, a putative RNA-dependent ATPase, shares extensive sequence homology with two other pre-mRNA splicing factors. *Nucleic Acids Res 18*:6447.

Cheng SC, Abelson J. 1987. Spliceosome assembly in yeast. *Genes & Dev 1*:1014–1027.

Cortes JJ, Sontheimer EJ, Seiwer SD, Steitz JA. 1993. Mutations in the conserved loop of human U5 snRNA generate the use of novel cryptic 5′ splice sites in vivo. *EMBO J 12*:5191–5200.

Couto JR, Tamm J, Parker R, Guthrie C. 1987. A *trans*-acting suppressor restores splicing of a yeast intron with a branch point mutation. *Genes & Dev 1*:445–455.

Frank D, Guthrie C. 1992. An essential splicing factor, SLU7, mediates 3′ splice site choice in yeast. *Genes & Dev 6*:2112–2124.

Frank D, Patterson B, Guthrie C. 1992. Synthetic lethal mutations suggest interactions between U5 small nuclear RNA and four proteins required for the second step of splicing. *Mol Cell Biol 12*:5197–5205.

Gozani O, Patton JG, Reed R. 1994. A novel set of spliceosome-associated proteins and the essential splicing factor PSF bind stably to pre-mRNA prior to catalytic step II of the splicing reaction. *EMBO J 13*:3356–3367.

Green MR. 1991. Biochemical mechanisms of constitutive and regulated pre-mRNA splicing. *Annu Rev Cell Biol 7*:559–599.

Guthrie C. 1991. Messenger RNA splicing in yeast: Clues to why the spliceosome is a ribonucleoprotein. *Science 253*:157–163.

Guthrie C, Fink GR. 1991. *Guide to yeast genetics and molecular biology*. San Diego: Academic Press.

Hodges PE, Jackson SP, Brown JD, Beggs JD. 1995. Extraordinary sequence conservation of the PRP8 splicing factor. *YEAST 11*: 337–342.

Horowitz DS, Abelson J. 1993a. Stages in the second reaction of pre-mRNA splicing: The final step is ATP independent. *Genes & Dev 7*:320–329.

Horowitz DS, Abelson J. 1993b. A U5 small nuclear ribonucleoprotein particle protein involved only in the second step of pre-mRNA splicing in *Saccharomyces cerevisiae*. *Mol Cell Biol 13*:2959–2970.

Jackson SP, Lossky M, Beggs JD. 1988. Cloning of the RNA8 gene of *Saccharomyces cerevisiae*, detection of the RNA8 protein, and demonstration that it is essential for nuclear pre-mRNA splicing. *Mol Cell Biol 8*:1067–1075.

Jones SH, Frank DN, Guthrie C. 1995. Characterization and functional ordering of Slu7p and Prp17p during the second step of pre-mRNA splicing in yeast. *Proc Natl Acad Sci USA*. Forthcoming.

Kim SH, Lin RJ. 1993. Pre-mRNA splicing within an assembled yeast spliceosome requires an RNA-dependent ATPase and ATP hydrolysis. *Proc Natl Acad Sci USA 90*:888–892.

Lamond AI, Konarska MM, Sharp PA. 1987. A mutational analysis of spliceosome assembly: Evidence for splice site collaboration during spliceosome formation. *Genes & Dev 1*:532–543.

Last RL, Maddock JR, Woolford JL Jr. 1987. Evidence for related functions of the RNA genes of *Saccharomyces cerevisiae*. *Genetics 117*:619–631.

Liao XC, Tang J, Rosbash M. 1993. An enhancer screen identifies a gene that encodes the yeast U1 snRNP A protein: Implications for snRNP protein function in pre-mRNA splicing. *Genes & Dev 7*:419–428.

Lin RJ, Newman AJ, Cheng SC, Abelson J. 1985. Yeast mRNA splicing in vitro. *J Biol Chem 260*:14780–14792.

Lossky M, Anderson GJ, Jackson SP, Beggs J. 1987. Identification of a yeast snRNP protein and detection of snRNP–snRNP interactions. *Cell 51*:1019–1026.

Lustig AJ, Lin RJ, Abelson J. 1986. The yeast RNA gene products are essential for mRNA splicing in vitro. *Cell 47*:953–963.

Madhani HD, Guthrie C. 1994a. Dynamic RNA–RNA interactions in the spliceosome. *Annu Rev Genet 28*:1–26.

Madhani HD, Guthrie C. 1994b. Genetic interactions between the yeast RNA helicase homolog Prp16 and spliceosomal snRNAs identify candidate ligands for the Prp16 RNA-dependent ATPase. *Genetics 137*:677–687.

Moore MJ, Query CC, Sharp PA. 1993. Splicing of precursors to mRNA by the spliceosome. In: Gesteland RF, Atkins JF, eds. *The RNA world*. Plainview, New York: Cold Spring Harbor Laboratory Press. pp 303–358.

Newman A, Norman C. 1991. Mutations in yeast U5 snRNA alter the specificity of 5′ splice-site cleavage. *Cell 65*:115–123.

Newman AJ, Norman C. 1992. U5 snRNA interacts with exon sequences at 5′ and 3′ splice sites. *Cell 68*:743–754.

Parker R, Siliciano PG. 1993. Evidence for an essential non-Watson-Crick interaction between the first and last nucleotides of a nuclear pre-mRNA intron. *Nature 361*:660–662.

Pinto AL, Steitz JA. 1989. The mammalian analogue of the yeast PRP8

splicing protein is present in the U4/5/6 small nuclear ribonucleoprotein particle and the spliceosome. *Proc Natl Acad Sci USA 86*:8742–8746.

Reed R. 1989. The organization of 3′ splice-site sequences in mammalian introns. *Genes & Dev 3*:2113–2123.

Reed R, Maniatis T. 1985. Intron sequences involved in lariat formation during pre-mRNA splicing. *Cell 41*:95–105.

Ruby SW, Chang TH, Abelson J. 1993. Four yeast spliceosomal proteins (PRP5, PRP9, PRP11, and PRP21) interact to promote U2 snRNP binding to pre-mRNA. *Genes & Dev 7*:1909–1925.

Ruskin B, Green MR. 1985. Role of the 3′ splice site consensus sequence in mammalian pre-mRNA splicing. *Nature 317*:732–734.

Rymond B, Rosbash M. 1992. Yeast pre-mRNA splicing. In: Jones EW, Pringle JR, Broach JR, eds. *The molecular and cellular biology of the yeast Saccharomyces*. Plainview, New York: Cold Spring Harbor Laboratory Press. pp 143–192.

Rymond BC, Rosbash M. 1985. Cleavage of 5′ splice site and lariat formation are independent of 3′ splice site in yeast mRNA splicing. *Nature 317*:735–737.

Rymond BC, Torrey DD, Rosbash M. 1987. A novel role for the 3′ region of introns in pre-mRNA splicing of *Saccharomyces cerevisiae*. *Genes & Dev 1*:238–246.

Schmid SR, Linder P. 1992. D-E-A-D protein family of putative RNA helicases. *Mol Microbiol 6*:283–291.

Schwer B, Guthrie C. 1991. PRP16 is an RNA-dependent ATPase that interacts transiently with the spliceosome. *Nature 349*:494–499.

Schwer B, Guthrie C. 1992a. A conformational rearrangement in the spliceosome is dependent on PRP16 and ATP hydrolysis. *EMBO J 11*:5033–5039.

Schwer B, Guthrie C. 1992b. A dominant negative mutation in a spliceosomal ATPase affects ATP hydrolysis but not binding to the spliceosome. *Mol Cell Biol 12*:3540–3547.

Shannon KW, Guthrie C. 1991. Suppressors of a U4 snRNA mutation define a novel U6 snRNP protein with RNA-binding motifs. *Genes & Dev 5*:773–785.

Sikorski RS, Hieter P. 1989. A system of shuttle vectors and yeast host strains designed for efficient manipulation of DNA in *Saccharomyces cerevisiae*. *Genetics 122*:19–27.

Sontheimer EJ, Steitz JA. 1993. The U5 and U6 small nuclear RNAs as active site components of the spliceosome. *Science 262*:1989–1996.

Teigelkamp S, Newman AJ, Beggs JD. 1995a. Extensive interactions of PRP8 protein with the 5′ and 3′ splice sites during splicing suggest a role in stabilization of exon alignment by U5 snRNA. *EMBO J 14*:2602–2612.

Teigelkamp S, Whittaker E, Beggs JD. 1995b. Interaction of the yeast splicing factor PRP8 with substrate RNA during both steps of splicing. *Nucleic Acids Res 23*:320–326.

Umen JG, Guthrie C. 1995. A novel role for a U5 snRNP protein in 3′ splice site selection. *Genes & Dev 9*:855–868.

Vijayraghavan U, Abelson J. 1990. PRP18, a protein required for the second reaction in pre-mRNA splicing. *Mol Cell Biol 10*:324–332.

Vijayraghavan U, Company M, Abelson J. 1989. Isolation and characterization of pre-mRNA splicing mutants of *Saccharomyces cerevisiae*. *Genes & Dev 3*:1206–1216.

Wells SE, Ares M Jr. 1994. Interactions between highly conserved U2 small nuclear RNA structures and Prp5p, Prp9p, Prp11p, and Prp21p proteins are required to ensure integrity of the U2 small nuclear ribonucleoprotein in *Saccharomyces cerevisiae*. *Mol Cell Biol 14*:6337–6349.

Whittaker E, Lossky M, Beggs JD. 1990. Affinity purification of spliceosomes reveals that the precursor RNA processing protein PRP8, a protein in the U5 small nuclear ribonucleoprotein particle, is a component of yeast spliceosomes. *Proc Natl Acad Sci USA 87*:2216–2219.

Wyatt JR, Sontheimer EJ, Steitz JA. 1992. Site-specific cross-linking of mammalian U5 snRNP to the 5′ splice site before the first step of pre-mRNA splicing. *Genes & Dev 6*:2542–2553.

Zamore PD, Green MR. 1991. Biochemical characterization of U2 snRNP auxiliary factor: An essential pre-mRNA splicing factor with a novel intranuclear distribution. *EMBO J 10*:207–214.

Zhuang Y, Weiner AM. 1990. The conserved dinucleotide AG of the 3′ splice site may be recognized twice during in vitro splicing of mammalian mRNA precursors. *Gene 90*:263–269.